Equilibrium Control of Crystal Thickness and Melting Point through Block Copolymerization

Li-Bong W. Lee† and Richard A. Register*

Department of Chemical Engineering, Princeton University, Princeton, New Jersey 08544-5263

Received May 2, 2004; Revised Manuscript Received July 15, 2004

ABSTRACT: While the crystal thickness and melting point in crystallizable homopolymers are kinetically controlled, an equilibrium degree of chain folding is predicted for crystalline−amorphous block copolymers. We demonstrate this effect in a series of diblock copolymers of hydrogenated polynorbornene and hydrogenated poly(ethylidene norbornene), hPN/hPEN, where the hPN block is induced to fold as many as four times by the attachment of progressively longer amorphous blocks. These diblocks all crystallize from homogeneous melts, permitting the equilibrium solid-state structure to be approached. Increased chain folding produces thinner crystals with lower melting points; these stable melting points can be reproducibly tuned over a 30 °C range through the choice of the amorphous block length. Finally, the end group on the hPN chain is shown to influence the melting point as well through its impact on the crystal surface energy.

Introduction

In semicrystalline homopolymers of all but the lowest molecular weights, crystal thickness and melting point are kinetically set; the predominant crystal stem length, and the extent of chain folding, are determined through the processing history of the material (such as crystallization temperature or rate and postcrystallization annealing).[1] In statistical copolymers, a broad distribution of crystal thicknesses and melting points is generally obtained, reflecting both kinetic constraints and the broad distribution of crystallizable sequence lengths within the ensemble.[2−4] For block copolymers of uniform chain length, however, there is a longstanding theoretical prediction,[5−7] due originally to DiMarzio, Guttman, and Hoffman (DGH),[5] that the crystalline domains should be of an essentially uniform thickness, with a crystal stem length (degree of chain folding) determined not through crystallization kinetics but set via equilibrium considerations.

Fundamentally, this degree of chain folding is set through a compromise between the extended-chain conformation favored by the crystalline block at equilibrium and the random coil conformation favored by the amorphous block. It is presumed that the lamellar morphology favored by homopolymers is retained in the block copolymer, thus producing a morphology consisting of alternating crystalline and amorphous regions for any ratio of crystalline and amorphous block lengths, as schematically illustrated in Figure 1a. Since the two blocks are covalently connected, each must occupy the same area on both sides of the lamellar interface while filling space at bulk density. To meet this requirement, the crystalline block adopts an equilibrium degree of chain folding to increase its area per chain at the interface, while the amorphous block adopts a distorted random coil conformation or even a strongly stretched conformation for very short blocks.[8] The longer the amorphous block, the more folded the crystalline block becomes. The scaling prediction of the DGH theory[5] for the lamellar repeat distance d illustrated in Figure 1a is

$$d \sim N_t N_a^{-1/3} \quad (1)$$

where N_t and N_a are the degrees of polymerization of the entire diblock and the amorphous block. Though different theoretical treatments presented subsequently yield somewhat different exponents on N_a (−5/12 in ref 6, −6/11 in ref 7), the scaling form of eq 1 is preserved.

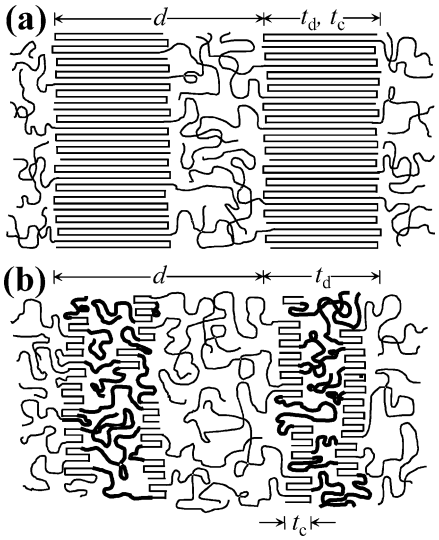

Figure 1. Schematic diagrams of the lamellar morphology of diblock copolymers crystallizing from single-phase melts. (a, top) Hypothetical morphology[5] for copolymers with a highly crystalline defect-free block, where tight folding and full crystallization yield a crystal thickness t_c equal to the crystallizable block domain thickness t_d. (b, bottom) Actual morphology for polymers with defective crystallizable blocks,[11] where t_c is limited to a value below t_d. Horizontal lines represent crystal stems; thin curves represent amorphous block chains; thicker curves in (b) represent the amorphous portion of the crystallizable block, containing both defects and topologically frustrated crystallizable segments.[4]

† Present address: ExxonMobil Upstream Research Co., P.O. Box 2189, Houston, TX 77252.

* Author for correspondence: e-mail register@princeton.edu.

10.1021/ma049143m CCC: $27.50
Published on Web 08/27/2004

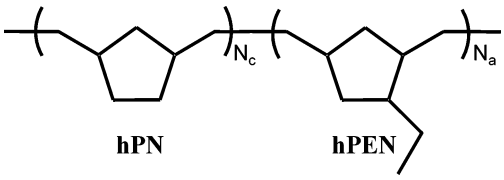

Figure 2. Repeat structure of hPN/hPEN diblocks; end groups not shown.

In practice, realization of this equilibrium control of crystal thickness (and melting point) through variation in the amorphous block length is a challenge. One requirement is that the crystallizable block be free from chain defects that would limit the stem length. This requirement is *not* met by one of the more commonly employed crystallizable blocks: hydrogenated high-1,4 polybutadiene, where the polybutadiene is synthesized by anionic polymerization. The hydrogenated product is structurally identical to a statistical ethylene−butene copolymer containing 8 wt % butene.[4,9] Indeed, block copolymers containing hydrogenated polybutadiene[10−12] show a broad distribution of crystal thicknesses[11,12] at room temperature, averaging $t_c \approx 5$ nm. Thus, when the blocks are sufficiently long and d sufficiently large, several crystals can be accommodated within the thickness of the crystallizable block domain t_d, with their thicknesses t_c set by the defect content, as shown in Figure 1b.

Another requirement is that the material is not kinetically constrained in adopting the equilibrium structure shown in Figure 1a, as might occur if the blocks were microphase-separated in the melt. Such a situation commonly occurs in polymers containing poly(ethylene oxide) blocks, PEO, which exhibit a large Flory interaction parameter (χ) against the nonpolar amorphous blocks with which they are commonly paired.[8,13−20] Achieving the equilibrium structure is particularly difficult when the crystallizable block forms discrete domains in the melt (spheres, cylinders),[14] but it is for precisely such cases—where the amorphous block is long relative to the crystalline block—that the extent of chain folding induced by the amorphous block is predicted to be greatest and for which eq 1 was developed. Even in diblocks comprised only of saturated hydrocarbons, melt microphase separation will still occur when the molecular weights are sufficiently large, such that χN_t exceeds that at the order−disorder transition.[21] Even for near-symmetric diblocks, where the melt morphology is lamellar, the solid-state morphology does not correspond to that in Figure 1 if crystallization is confined to within the preexisting lamellae; the crystal stems lie parallel to the microdomain interfaces rather than perpendicular.[12,22−24]

Here, we use ring-opening metathesis polymerization to synthesize well-defined block copolymers of norbornene and ethylidene norbornene, which after hydrogenation are saturated hydrocarbon polymers with the chemical structure shown schematically in Figure 2. Hydrogenated polynorbornene, hPN, is a highly crystalline polymer[25−27] with an equilibrium melting point of 156 °C, while hydrogenated poly(ethylidene norbornene), hPEN, is amorphous with a glass transition temperature[28] of 15 °C. The chemical similarity between the two blocks yields a small χ, leading to homogeneous melts even at relatively high molecular weights, permitting the hypothetical morphology illustrated in Figure 1a to be approached in practice.

Experimental Section

ROMP. Polymerizations were performed in flame-dried glassware under a nitrogen atmosphere (<1 ppm of O_2, H_2O) in an Innovative Technology glovebox. Toluene used as the solvent for polymerizations was dried over sodium benzophenone ketyl, degassed by freeze−pump−thaw cycles, and vacuum-transferred prior to use. Norbornene (Aldrich, 99%), 5-ethylidene-2-norbornene (99%, mixture of endo and exo), and PMe_3 (Aldrich, 97%) were dried over sodium, while propionaldehyde (97%) was dried over $CaSO_4$; all were then degassed and vacuum-transferred. The ROMP initiator, 2,6-diisopropylphenylimidoneophylidenemolybdenum(VI) bis(*tert*-butoxide), a "Schrock-type" catalyst, was used as received (Strem Chemicals), as was benzaldehyde (Aldrich, 99.5%, Sure-Seal). Polymerizations were conducted at room temperature, at 0.04 g monomer/mL solution, with a monomer:initiator ratio calculated to produce the desired molecular weight at complete monomer conversion. A 5:1 molar ratio of PMe_3:Mo was employed to suppress the formation of a subsidiary amount of very high molecular weight polymer.[28] PN homopolymers of varying molecular weights were synthesized by varying the monomer:initiator ratio, terminating with 100 equiv of benzaldehyde after 1 h of polymerization. Diblocks were synthesized in either order: norbornene block first or ethylidene norbornene block first. Polymerizations proceed to >99.9% conversion within the 1 h allotted for each block,[29] ensuring neglible incorporation of the first monomer into the second block. Prior to addition of the second monomer charge, a sample of the first block was removed for characterization, terminating with a large excess of the same aldehyde used subsequently to terminate the diblock. One hour after addition of the second monomer, the reaction was terminated with 100 equiv of benzaldehyde or propionaldehyde. All polymers were isolated by twice precipitating into a 2:1 methanol:acetone mixture and vacuum-drying.

Hydrogenation. Polymers were dissolved at 2 wt % in an 80/20 mixture of cyclohexane/tetrahydrofuran and hydrogenated at 100 °C and 400−600 psig of H_2 (BOC Gases, 99.999%). The catalyst employed was 5 wt % reduced Pd on $CaCO_3$ (Strem, used as received), typically added at a 2:1 wt ratio of catalyst (including support) to polymer. Hydrogenations were typically carried out for 48 h; progress of the reaction was periodically monitored by analyzing aliquots by infrared spectrometry (Nicolet 730), and the reaction continued until the *trans*-C═C band at 965 cm^{-1} was no longer detectable, which for the hPN homopolymer corresponds to a maximum of 0.25% residual unsaturation (detectability limit). The catalyst was separated from the polymer solution by hot filtration, and the polymer was isolated by precipitation into methanol and dried in a vacuum oven. The crystalline nature of hPN precludes post-hydrogenation examination by room temperature gel permeation chromatography; however, homopoly(ethylidene norbornene) saturated in our laboratory under identical conditions shows no backbone rearrangements,[28] and PEN has even poorer thermooxidative stability than PN, so we expect that no backbone rearrangements occurred in the diblocks upon hydrogenation. Compositions and molecular weights measured on the unsaturated precursors were adjusted (by 2.02 g/mol per PN repeat unit, 4.03 g/mol per PEN repeat unit) to correspond to those for the hydrogenated products; all numerical values reported herein correspond to fully saturated polymers.

Characterization. Polymer molecular weights and polydispersity indices were determined by gel permeation chromatography (GPC) in toluene,[28] with columns calibrated against polystyrene standards. To convert these "polystyrene equivalent" values to true molecular weights, they were divided by 2.2 for polynorbornene[30] or 2.12 for poly(ethylidene norbornene).[28] All block copolymers had polydispersities of 1.04−1.05, with no detectable terminated first block. For the block copolymers, M_n of the first block was determined by GPC, and the diblock molecular weight was determined from this value and the diblock's composition. The norbornene weight fraction, always close to the synthesis target, was measured

Table 1. Characteristics of Diblock Copolymers Studied[a]

block copolymer	f_{hPN}	block M_n (kg/mol)	M_w/M_n (1st block/diblock)	q^* (nm^{-1})	d (nm)	t_d (nm)	n (no. of folds)	T_m (°C)	ΔH_f (J/g)	$w_{c,hPN}$	t_c (nm)
hPN/hPEN 6/2	0.71	5.6/2.3	1.05/1.04	0.238	26	18	1	115	46	0.75	14
hPN/hPEN 6/5	0.51	5.6/5.3	1.05/1.04	0.200	31	16	1	109	30	0.68	10
hPN/hPEN 6/17	0.26	5.8/16.7	1.06/1.04	0.139	45	11	2	104	15	0.67	7.4
hPN/hPEN 5/33	0.13	5.1/32.8	1.05/1.04	0.128	49	6.2	4	96	6.6	0.59	3.5
hPEN/hPN_{BA} 2/6	0.74	2.1/5.8	1.11/1.04	0.192	33	24	<1	122	54	0.85	20
hPEN/hPN_{PA} 2/5	0.72	2.1/5.3	1.11/1.05	0.214	29	21	<1	119	50	0.81	17
hPEN/hPN_{PA} 6/6	0.48	5.9/5.5	1.07/1.05	0.193	33	15	1	116	34	0.82	12
hPEN/hPN_{PA} 21/6	0.22	20.7/5.8	1.06/1.05	0.114	55	11	2	109	13	0.69	7.8

[a] Morphological characteristics (q^*, d, n, T_m, ΔH_f, $w_{c,hPN}$) were determined on specimens slow-cooled from the melt, at 1°C/min (DSC) or 0.5 °C/min (SAXS), then annealed for 1−2 h at 10−15 °C below T_m. However, virtually identical values were measured on slow-cooled but unannealed specimens.

precisely by ^1H NMR in C_6D_6 (General Electric QE 300), using the area of the ethylidene methyl protons relative to the total alkyl region.[26]

Differential scanning calorimetry (DSC) data were acquired with a Perkin-Elmer DSC-7 calibrated with indium and mercury, scanning at 10 °C/min. Pressure−volume−temperature measurements were performed by Dr. Gregory T. Dee of DuPont Central Research & Development using a Gnomix PVT apparatus[31] and determining room temperature density via an autopycnometer. Small-angle X-ray scattering (SAXS) patterns were acquired with a Kratky camera equipped with hotstage.[32] Data were corrected for empty beam scattering and absorption, normalized for sample thickness, placed on an absolute intensity scale with a polyethylene strip traceable to a Kratky Lupolen standard, desmeared, and the thermal density fluctuation background subtracted.[33] Absolute SAXS intensities I are plotted against $q = (4\pi/\lambda)\sin\theta$, where λ is the Cu Kα X-ray wavelength and θ half the scattering angle.

Results and Discussion

To critically test eq 1's prediction of increased chain folding with increasing amorphous block length, all the diblock copolymers described in this paper were synthesized to have a near-constant hPN block molecular weight (ca. 6 kg/mol), but with hPEN blocks ranging from 2 to 33 kg/mol, as listed in Table 1, where f_{hPN} is the weight fraction of hPN in each diblock. Though the diblocks can be synthesized equally well in either order (norbornene or ethylidene norbornene block first), the sequence determines the chemical identity of the monomeric end group attached to the hPN block, which we will show subsequently to be important. Consequently, block copolymers are denoted throughout according to the sequence of block synthesis, with the block molecular weights indicated to the nearest kg/mol; for example, hPN/hPEN 6/2 was polymerized norbornene block first (6 kg/mol) and ethylidene norbornene block second (2 kg/mol). When norbornene was the second block, the identity of the terminating agent (propionaldehyde, PA; benzaldehyde, BA) is indicated by a subscript, e.g., hPEN/hPN_{PA} 21/6.

At 6 kg/mol, narrow-distribution hPN homopolymers readily form extended-chain crystals without special thermal treatment. Figure 3a presents SAXS data for two hPN homopolymers, having molecular weights of 4 and 12 kg/mol, after cooling from the melt to room temperature at 8 °C/min. Both show a series of sharp peaks integrally spaced in q, characteristic of a highly regular lamellar structure. The interdomain spacing d can be determined from the position q^* of the first-order peak in a plot of q^2I vs q according to Bragg's law, $d = 2\pi/q^*$; for hPN 4, $d = 28$ nm, while for hPN 12, $d = 43$ nm. These values may be compared with the lengths L of the fully extended hPN chains, knowing each polymer's molecular weight and the hPN crystal structure,[26,27] which has a c-axis dimension (two hPN repeats) of 1.242 nm; X-ray diffraction[26] confirmed that the block copolymers and low molecular weight homopolymers examined here contain the same room temperature hPN polymorph as high molecular weight hPN. For hPN 4, $L = 27$ nm, while for hPN 12, $L = 78$ nm (calculated from M_n). Thus, hPN 4 forms extended-chain crystals following this thermal history, while hPN 12 forms once-folded ($n = 1$) crystals. This comparison implicitly assumes 100% crystallinity (crystal thickness $t_c = t_d$, and $t_d = d$ for homopolymers; see Figure 1a), though high-molecular-weight hPN homopolymer is only 70−80% crystalline by X-ray diffraction;[26,27] however, the minor fraction of amorphous segments in hPN

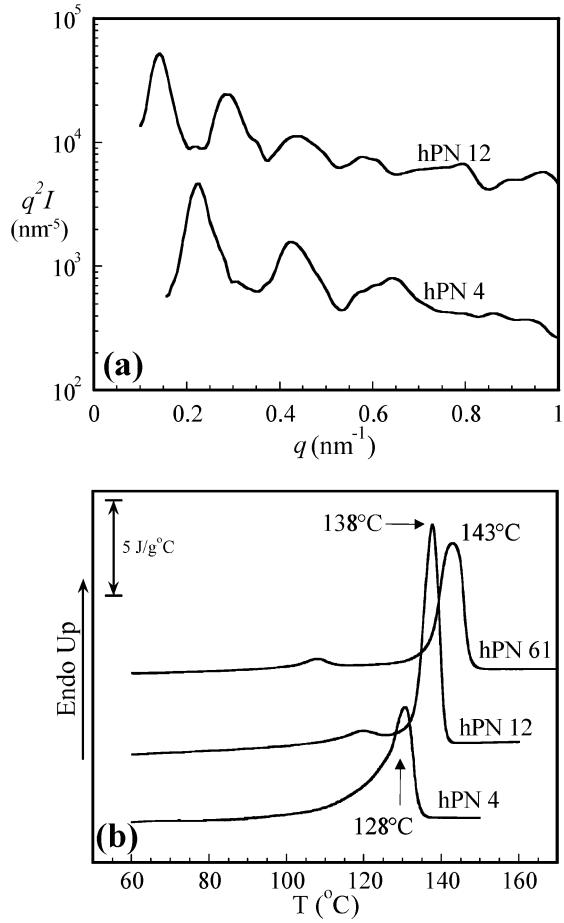

Figure 3. Data for three hPN homopolymers: hPN 4 (M_n = 4.1 kg/mol, M_w/M_n = 1.13), hPN 12 (M_n = 12.1 kg/mol, M_w/M_n = 1.03), and hPN 61 (M_n = 61 kg/mol, M_w/M_n = 1.11). (a) SAXS patterns obtained at room temperature on specimens cooled from the melt at 8 °C/min. Intensity for hPN 12 multiplied by 10 for clarity. (b) DSC heating thermograms obtained after cooling from the melt to room temperature at 10 °C/min. Peak melting temperature (T_m) indicated.

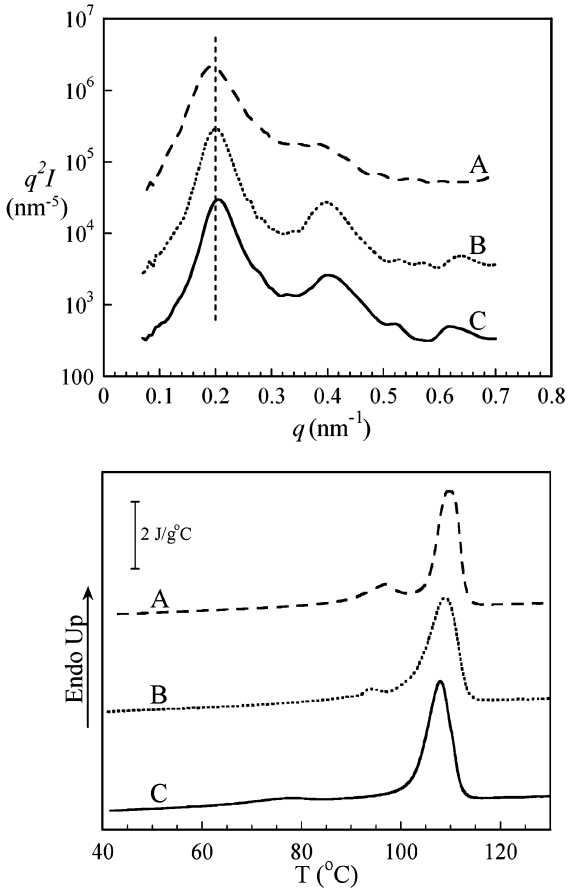

Figure 4. (top) Room temperature SAXS patterns for hPN/hPEN 6/5 taken following three different thermal histories, shifted successively upward by a decade in intensity (vs history C) for clarity. (bottom) Corresponding DSC traces (heating, 10 °C/min). History A: quenched from the melt in liquid nitrogen, then held at 90 °C for 2 h; B: cooled at 0.5−1 °C/min from the melt to room temperature, then held at 90 °C for 2 h; C: as B, but cooled at 8−10 °C/min, no anneal.

4 and 12 must also be highly extended, since they are part of unfolded or once-folded chains and cannot relax to a random coil conformation without producing a segment density in the amorphous phase which exceeds that in the crystal. The quantitative agreement between d and $L/(n + 1)$, where n is the number of folds in the hPN block, confirms this assumption. Figure 3b shows DSC traces for hPN 4 and 12, and a high molecular weight hPN, demonstrating the expected increase in melting point T_m with crystal thickness t_c.

The Flory interaction parameter χ is found to be small in the hPN/hPEN system. A near-symmetric hPN/hPEN 34/31 diblock shows a featureless SAXS pattern[26] in the melt (140 °C), although the mass densities of molten hPN and hPEN at 140 °C yield an electron density difference between the two of 8 e$^-$/nm^3—a contrast easily sufficient for our SAXS apparatus to detect the peak from an ordered diblock, were one present.[34] With the mean-field value of $\chi N_t = 10.5$ at the order−disorder transition for a symmetric diblock,[21] this yields $\chi < 0.02$ for the hPN/hPEN system (and possibly much less, as we have yet to synthesize an hPN/hPEN diblock which is microphase-separated in the melt).

Figure 4 shows SAXS patterns and DSC thermograms for hPN/hPEN 6/5, following three very different thermal histories described in the caption. All three histories produce essentially identical values for q^* (0.20 nm^{-1})

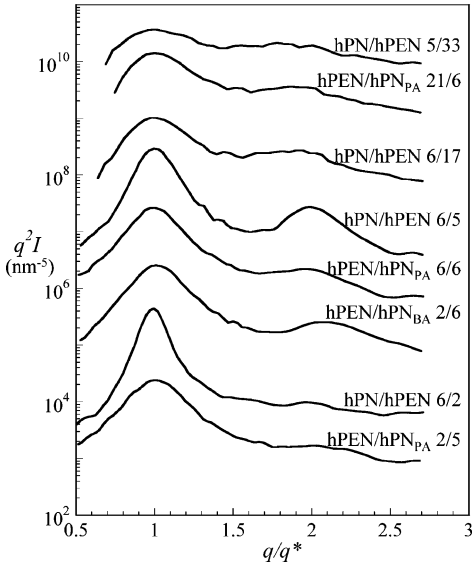

Figure 5. Composite plot of room temperature SAXS data for all diblocks examined. The q axis is scaled as q/q^* to highlight the existence of peaks in a q ratio of 1:2, as expected for lamellar diblocks. The intensities for each curve (above that for hPEN/hPN$_{PA}$ 2/5) are shifted by successive factors of a decade apiece to prevent overlap.

and T_m (109 °C), consistent with the idea of an equilibrium domain spacing and degree of chain folding. Using the bulk density of semicrystalline hPN (0.995 g/cm^3) and hPEN (0.939 g/cm^3) at room temperature,[26] coupled with the mass fraction of hPN in the diblock, f_{hPN}, the thickness of the hPN domain t_d (see Figure 1) is calculated as 16 nm. By comparison, the fully extended length of the hPN block is calculated as 36 nm, indicating that the 6 kg/mol hPN block in hPN/hPEN 6/5 is once-folded ($n = 1$), vs $n = 0$ for hPN 4 and $n = 1$ for hPN 12 (corresponding to the same crystal thickness as an unfolded hPN homopolymer at 6 kg/mol) cooled at 8 °C/min. These results clearly demonstrate that hPN/hPEN 6/5 forms more-folded crystals than it would were the amorphous hPEN block not attached. Moreover, the insensitivity to thermal history strongly suggests that the $n = 1$ crystals formed in the diblock correspond to the equilibrium state. Indeed, we attempted to induce the chains to unfold through "self-seeded" crystallization,[14] by heating to a temperature just below the final melting point, followed by an isothermal crystallization at a lower temperature; however, no substantial increase in T_m, which would accompany a transition from $n = 1$ to $n = 0$, was observed for any combination of heating and crystallization temperatures.

Figure 5 shows SAXS patterns for all the diblocks in Table 1, after cooling from the melt at 0.5 °C/min. To facilitate comparison between the patterns, the abscissa for each has been normalized by q^*. All SAXS patterns show peaks in a q ratio of 1:2, confirming that a lamellar morphology is adopted for all compositions ($f_{hPN} = 0.13$−0.73), though attenuation of the second-order peak and broadening of the first-order peak indicate reduced regularity in the interdomain spacing at the highest and lowest contents of hPN.

Figure 6 plots the domain spacings for the block copolymers in the expected scaling form, where N_t and N_a were calculated with the actual molecular weights of the hPN and hPEN mers (96.17 and 124.23 g/mol, respectively). Our data conform well to the DGH theory,

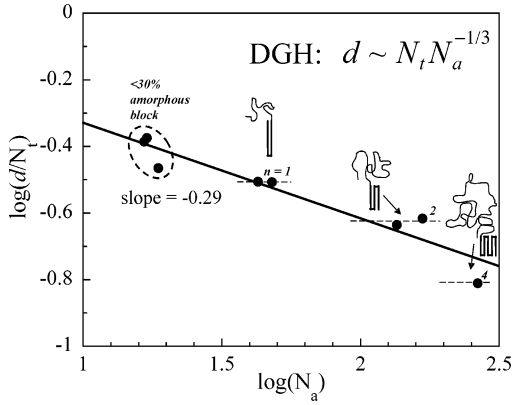

Figure 6. Interlamellar spacings d for hPN/hPEN diblocks, plotted in the scaling form suggested by the DGH theory. Each point represents a different block copolymer (all with hPN block M_n near 6 kg/mol). Dashed horizontal lines represent plateaus corresponding to a discrete number of folds n of the hPN block, as indicated in the schematic structures.

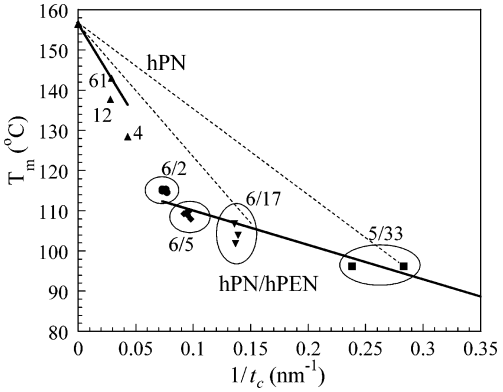

Figure 7. Peak melting temperatures for hPN homopolymers (upper left of figure) and four hPN/hPEN block copolymers synthesized norbornene block first (lower half of figure), plotted against reciprocal crystal thickness. Numbers indicate M_n values in kg/mol. The solid line at the upper left represents the Gibbs−Thomson relationship for the homopolymer hPN 61. The lower solid curve, for the block copolymers, is a guide to the eye, as are the dashed curves; see text for explanation.

with the best-fit line showing a slope (−0.29) close to the prediction of −1/3 in eq 1. This result is fairly insensitive to reasonable choices of what constitutes a repeat unit in the calculation of N_t and N_a; for example, if a uniform mer molecular weight is employed (e.g., 100 g/mol for both hPN and hPEN) instead,[26] the best-fit slope is −0.34. However, we note that the small number of points in Figure 6 precludes us from assessing whether the dependence of d/N_t truly follows a power law in N_a.

Close examination of the data in Figure 6 reveals a set of plateaus, rather than a continuous decline in d/N_t with increasing N_a. The number of folds per crystalline block (n), calculated as outlined above for hPN/hPEN 6/5 (as $n = (L/t_d) - 1$), is indicated next to each plateau. The polymers with the shortest hPEN blocks ($f_{hPN} > 0.7$) are difficult to classify; the two with the lowest values of N_a have calculated values of n close to 1/2, which would imply either that the end groups in these polymers are actually incorporated within the crystal or that each crystalline block domain contains two crystals across its thickness rather than one (a "bilayer" structure).[6] Tilt of the crystal stems away from the lamellar normal could also produce an apparent non-integral folding, though we have no independent evidence for such tilting. The polymer with the third smallest value of N_a (log N_a = 1.28) has a calculated value of n close to unity, yet exhibits d/N_t approximately 15% higher than observed for the other two polymers with $n = 1$. But for longer hPN blocks ($f_{hPN} < 0.6$), there is no ambiguity: clear "steps" are observed in d/N_t as N_a is increased, corresponding to increments in n. As N_a is increased, d simply increases proportionally (to N_t) until the amorphous block becomes sufficiently long that the crystalline block undergoes an extra fold, as illustrated schematically in Figure 6. The most closely related observation in the prior literature is that by Ryan et al.[14,35] on poly(ethylene oxide)/poly(butylene oxide) diblocks, PEO/PBO, of low molecular weight (M_n-(PEO) < 2000 g/mol); at these molecular weights, the diblocks crystallize from disordered melts, which should also permit the equilibrium structure to be approached. They found that increasing the amorphous block length at a fixed PEO molecular weight could induce a transition from an unfolded PEO block ($n = 0$) to a stable, once-folded PEO block ($n = 1$). Here, by choosing a system with a small χ, we are able to increase the degree of folding to at least $n = 4$ while still crystallizing from homogeneous melts, and there is no suggestion in Figure 6 that any limit on n has been reached. Thus, our results confirm the basic premise underlying the DGH theory—an equilibrium degree of chain folding which increases with the length of the amorphous block—and also reflect the discrete nature of chain folding at moderate n.

The reduction in crystal thickness with increasing N_a is also reflected in the peak melting temperature T_m determined by DSC (see Table 1). The hPN crystal thickness t_c can be calculated through d from the polymer's composition, the room temperature densities[26] of crystalline hPN (ρ_c = 1.005 g/cm^3), amorphous hPN (0.957 g/cm^3) and hPEN, and the degree of crystallinity of the hPN block, determined by DSC with reference to the heat of fusion of a perfect hPN crystal ΔH_{100} = 86 J/g, estimated from the measured heat of fusion for hPN 61 (65 J/g) and the degree of crystallinity from X-ray diffraction (w_c = 0.76).[27] Figure 7 plots T_m vs $1/t_c$ for four hPN/hPEN block copolymers, all synthesized hPN block first, as well as three hPN homopolymers. Focusing first on the latter, the solid line at the upper left in Figure 7 connects the measured point for hPN 61 (T_m, $1/t_c$) for a specimen cooled from the melt at 8−10 °C/min with the equilibrium melting temperature for hPN determined by Hoffman−Weeks extrapolation (T_m^0 = 156 °C, $1/t_c = 0$).[26,27] This line should be described by the Gibbs−Thomson equation, written here for lamellae of large lateral extent:[36]

$$T_m = T_m^0(1 - 2\sigma/\Delta H_{100}\rho_c t_c) \qquad (2)$$

where σ is the crystal surface energy. The slope of this line yields σ = 0.045 J/m^2, using ρ_c = 0.971 g/cm^3 at 150 °C.[26] Points for hPN 12 and hPN 4, determined from the data in Figure 3, are also plotted in Figure 7; for these lower molecular weight homopolymers, T_m lies systematically below the line for hPN 61 but well above the values for the block copolymers which we now discuss. The symbols contained within each of the four ovals in Figure 7 represent specimens of the same block copolymer with different thermal histories. For the diblocks with higher N_t (>200), quenching from the melt into liquid nitrogen typically produced a featureless

SAXS pattern, though crystallinity could be developed by reheating to ≈20 °C below T_m and holding for 1−2 h. These extreme thermal histories (slow-cooled vs quenched) are shown as the two points for hPN/hPEN 5/33.

The block copolymers do not follow the same T_m vs $1/t_c$ line as hPN 61, which may reflect changes in σ across the series because the composition (hPN:hPEN ratio) differs for each block copolymer. The value of n also influences the surface energy directly; for $n = 0$, the crystal surface should consist principally of the end groups on the hPN block (one hPEN block and one monomeric end group, as discussed further below), while for increasing n, hPN folds will constitute an increasing fraction of the material at the crystal surface. Consequently, the block copolymers should not lie on a common curve, as the lower solid line in Figure 7 might suggest; rather, each block copolymer represents a single point on a line of *different* σ, corresponding to the crystal's surface composition, as indicated schematically by the dashed lines in Figure 7. (These dotted lines cannot be traversed in practice, since this would require a change in the crystal thickness while keeping the crystal surface composition constant.) The shallower slopes of the dashed lines in Figure 7 suggest that for the block copolymers σ can be as small as half its value for the hPN 61 homopolymer. The magnitude of this difference is surprisingly large, especially in view of the fact that the hPN/hPEN domain spacings (Figure 6) are well-described by the DGH theory, in which a constant σ is assumed. In principle, T_m should also be influenced by the fact that the hPN crystals melt into an impure melt, consisting of a large and variable fraction of hPEN segments; however, since both units belong to polymer chains, the contribution of this effect to the entropy of melting is expected to be small and is in fact in the opposite direction to the effect observed in Figure 7, where the slope of the dashed line is less steep for polymers containing a greater fraction of hPEN.

Note that the data in Figure 7 span 50 °C, demonstrating the broad T_m control which can be achieved through attachment of an amorphous block. This is partly a consequence of the small value of ΔH_{100} for hPN, which is closer to that for semiflexible polymers such as poly(*p*-phenylene sulfide)[37] and poly(ether ether ketone),[38] around 100 J/g, than for polymers such as poly(ethylene oxide), at 200 J/g.[35] Smaller melting point depressions are observed in PEO/PBO diblocks.[35] It is also worth noting that the fractional crystallinity of the hPN block, $w_{c,hPN}$, decreases as N_a, and hence n, is increased (see values in last column of Table 1). The first four diblocks in Table 1, all synthesized norbornene block first, have the same end groups on the hPN block; across these four polymers, to within the combined measurement error in f_{hPN} and ΔH_f, $w_{c,hPN}$ decreases by ≈0.05 for each additional fold. This crystallinity decrement corresponds to three hPN units per fold—a reasonable value for the number of hPN units necessary to form a fold, given the rigid cyclopentylene ring in the backbone.

A further test of the idea that the block copolymer T_m is strongly affected by σ may be made by varying the end groups on the hPN block. As discussed above, since the hPN blocks in our diblocks have only a few folds ($n = 1-4$), the hPN block's end groups should constitute a substantial fraction of the material at the crystal surface. One of these end groups is always the

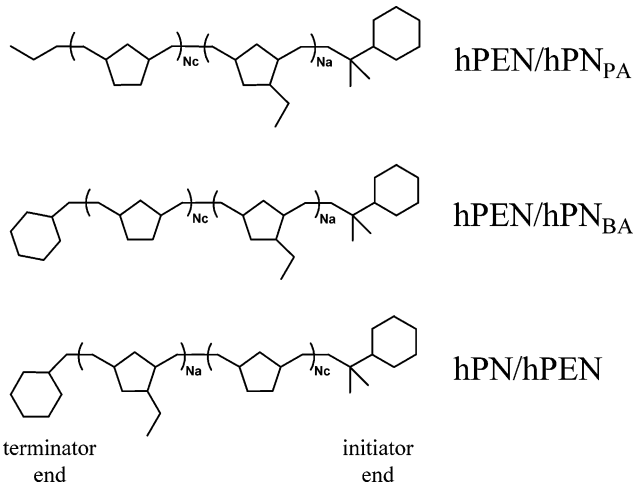

Figure 8. Chemical structures of the block copolymer systems used, with emphasis on the end groups: (top) the hPN block in hPEN/hPN$_{PA}$ diblocks is terminated with propionaldehyde; (middle) the hPN block in hPEN/hPN$_{BA}$ diblocks is terminated with benzaldehyde; (bottom) in hPN/hPEN diblocks, the norbornene block is polymerized first and thus bears the initiator ligand (isopropylphenyl) as an end group. Phenyl rings in end groups are hydrogenated to cyclohexyl rings under the conditions used here.[39]

hPEN block, but the identity of the other end group depends on the method of synthesis: whether the hPN block was synthesized first or second, and if the latter, what the identity of the terminating agent is. In this work, we have synthesized hPN/hPEN diblocks with three different types of end groups, as shown in Figure 8; the data in Figure 7 correspond only to diblocks of the "hPN/hPEN" type, where the hPN block bears a bulky cyclohexylisopropylidene group derived from the Schrock-type initiator ligand. Additional diblocks were synthesized with compositions similar to those for which data are shown in Figure 7, but with the hPN block synthesized second and with two different terminating agents, to produce the smaller cyclohexylmethylene (hPEN/hPN$_{BA}$) and propyl (hPEN/hPN$_{PA}$) end groups illustrated in Figure 8. The d vs N_a data for all these diblocks were previously included in the scaling plot (Figure 6), with no distinction between polymers of different end group, as no difference in d is observed. It is possible that the nature of the end groups could influence the precise values of N_a corresponding to the "steps" in Figure 6, where n increases to the next integer; that is, a bulkier end group might produce the same value of n at a slightly lower N_a than would a small end group. However, given the modest number of diblocks lying on each "step" in Figure 6, this effect, if present, is not resolvable.

On the other hand, an influence of the end group on T_m is readily detectable, as shown in Figure 9, where the dotted ovals enclose polymers of similar composition but different end groups (denoted by different symbols). Thus, the polymers within each oval have the same value of n (for $n \geq 1$). A small effect of end group on t_c is detectable, particularly when the hPEN block is only 2−5 kg/mol; a higher fractional crystallinity $w_{c,hPN}$ (see values in Table 1) is observed when the hPN block bears the smaller end group (hPEN/hPN$_{BA}$ and hPEN/hPN$_{PA}$, vs hPN/hPEN), leading to a larger t_c even at fixed d. A more pronounced end group effect is evident in T_m, as the diblocks with smaller end groups systematically

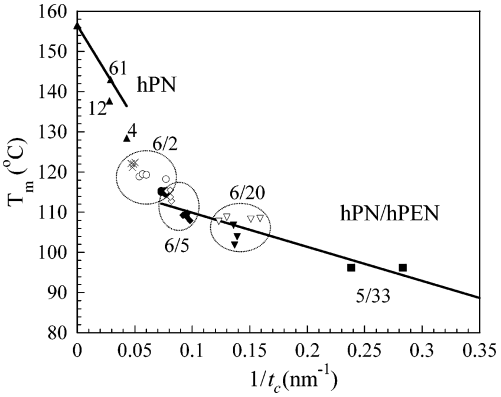

Figure 9. As Figure 7, but including data for block copolymers with all end group types. Dotted ovals surround diblocks of similar N_c and N_a but different end groups. Solid symbols correspond to hPN/hPEN diblocks (bulky end group); open symbols correspond to hPEN/hPN$_{PA}$ diblocks (smallest end group); × corresponds to the one hPEN/hPN$_{BA}$ diblock (intermediate). Numbers next to each oval indicate the approximate molecular weights of the hPN/hPEN blocks (in kg/mol), regardless of the actual order of block synthesis.

melt 4−6 °C higher than their analogues bearing the bulky cyclohexylisopropylidene end group. Only part of this effect can be attributed to the thicker crystals resulting from a higher degree of crystallinity; even at the same value of $1/t_c$ (see particularly the data for the polymers having hPEN end blocks near 20 kg/mol, where $n = 2$), the polymers with less bulky end groups have a higher T_m, consistent with a smaller value of the crystal surface energy σ. Thus, while the strongest modulation in T_m is achieved by changing the length of the amorphous block (and thus varying n), the choice of monomeric end group can also influence T_m through σ, as these end groups represent a significant fraction of the material at the crystal surface when n is modest.

Conclusions

The premise of the DiMarzio−Guttman−Hoffman theory—that the crystalline blocks in crystalline−amorphous diblock copolymers show an equilibrium degree of folding, increasing steadily with the length of the amorphous block—has been experimentally verified in the hPN/hPEN system, where a 6 kg/mol hPN block was induced to fold up to four times as the amorphous block increased in length. Reproducible interdomain spacings d and crystal thicknesses t_c were achieved for a range of thermal histories, strongly suggesting that these correspond closely to equilibrium values. The thinner crystals formed at higher degrees of folding show progressively lower melting temperatures T_m. However, the block copolymers do not follow the same T_m vs $1/t_c$ curve as hPN homopolymer due to the differences in composition at the crystal surfaces, which contain a large fraction of hPEN segments in the diblock case. Indeed, the melting point of the hPN crystals is found to be quite sensitive to the composition of the crystal surfaces; by varying the identity of the single monomeric hPN end group, at the opposite end of the hPN block from the hPEN block, a distinct effect on T_m is found.

Acknowledgment. This work was supported by the National Science Foundation through the Polymers Program (DMR-0220236), with partial support through the Princeton Center for Complex Materials (DMR-0213706). The authors thank Dr. Gregory T. Dee (DuPont) for the density measurements and John D. Hatjopoulos (Princeton) for complementary DSC measurements.

References and Notes

(1) Wunderlich, B. *Macromolecular Physics: Crystal Nucleation, Growth, Annealing*; Academic Press: New York, 1976; Vol. 2.
(2) Flory, P. J. *J. Chem. Phys.* **1949**, *17*, 223.
(3) Flory, P. J. *Trans. Faraday Soc.* **1955**, *51*, 548.
(4) Crist, B.; Howard, P. R. *Macromolecules* **1999**, *32*, 3057.
(5) DiMarzio, E. A.; Guttman, C. M.; Hoffman, J. D. *Macromolecules* **1980**, *13*, 1194.
(6) Whitmore, M. D.; Noolandi, J. *Macromolecules* **1988**, *21*, 1482.
(7) Vilgis, T. A.; Halperin, A. *Macromolecules* **1991**, *24*, 2090.
(8) Viras, K.; Kelarkis, A.; Havredaki, V.; Mai, S.-M.; Ryan, A. J.; Mistry, D.; Mingvanish, W.; MacKenzie, P.; Booth, C. *J. Phys. Chem. B* **2003**, *107*, 6946.
(9) Krigas, T. M.; Carella, J. M.; Struglinski, M. J.; Crist, B.; Graessley, W. W. *J. Polym. Sci., Polym. Phys. Ed.* **1985**, *23*, 589.
(10) Douzinas, K. C.; Cohen, R. E.; Halasa, A. F. *Macromolecules* **1991**, *24*, 4457.
(11) Rangarajan, P.; Register, R. A.; Fetters, L. J. *Macromolecules* **1993**, *26*, 4640.
(12) Hamley, I. W.; Fairclough, J. P. A.; Terrill, N. J.; Ryan, A. J.; Lipic, M.; Bates, F. S.; Towns-Andrews, E. *Macromolecules* **1996**, *29*, 8835.
(13) Gervais, M.; Gallot, B. *Makromol. Chem.* **1977**, *178*, 1577.
(14) Ryan, A. J.; Fairclough, J. P. A.; Hamley, I. W.; Mai, S.-M.; Booth, C. *Macromolecules* **1997**, *30*, 1723.
(15) Reiter, G.; Castelein, G.; Sommer, J.-U.; Röttele, A.; Thurn-Albrecht, T. *Phys. Rev. Lett.* **2001**, *87*, 226101.
(16) Chen, H.-L.; Wu, J.-C.; Lin, T.-L.; Lin, J. S. *Macromolecules* **2001**, *34*, 6936.
(17) Hong, S.; Yang, L.; MacKnight, W. J.; Gido, S. P. *Macromolecules* **2001**, *34*, 7009.
(18) Zhu, L.; Mimnaugh, B. R.; Ge, Q.; Quirk, R. P.; Cheng, S. Z. D.; Thomas, E. L.; Lotz, B.; Hsiao, B.; Yeh, F.; Liu, L. *Polymer* **2001**, *42*, 9121.
(19) Chaibundit, C.; Mingvanish, W.; Booth, C.; Mai, S.-M.; Turner, S. C.; Fairclough, J. P. A.; Ryan, A. J.; Pissis, P. *Macromolecules* **2002**, *35*, 4838.
(20) Xu, J.-T.; Turner, S. C.; Fairclough, J. P. A.; Mai, S.-M.; Ryan, A. J.; Chaibundit, C.; Booth, C. *Macromolecules* **2002**, *35*, 3614.
(21) Leibler, L. *Macromolecules* **1980**, *13*, 1602.
(22) Douzinas, K. C.; Cohen, R. E. *Macromolecules* **1992**, *25*, 5030.
(23) Cohen, R. E.; Bellare, A.; Drzewinski, M. A. *Macromolecules* **1994**, *27*, 2321.
(24) Loo, Y. L.; Register, R. A.; Ryan, A. J.; Dee, G. T. *Macromolecules* **2001**, *26*, 8968.
(25) Cataldo, F. *Polym. Int.* **1994**, *34*, 49.
(26) Lee, L.-B. W. Ph.D. Thesis, Princeton University, 2004.
(27) Lee, L.-B. W.; Register, R. A., manuscript in preparation.
(28) Trzaska, S. T.; Lee, L.-B. W.; Register, R. A. *Macromolecules* **2000**, *33*, 9215.
(29) Hatjopoulos, J. D.; Register, R. A. *ACS PMSE Proc.* **2004**, *91*, 971.
(30) Schrock, R. R.; Feldman, J.; Cannizzo, L. F.; Grubbs, R. H. *Macromolecules* **1987**, *20*, 1169.
(31) Zoller, P.; Bolli, P.; Pahud, V.; Ackermann, H. *Rev. Sci. Instrum.* **1976**, *47*, 948.
(32) Adams, J. L.; Quiram, D. J.; Graessley, W. W.; Register, R. A.; Marchand, G. R. *Macromolecules* **1996**, *29*, 2929.
(33) Register, R. A.; Bell, T. R. *J. Polym. Sci., Part B: Polym. Phys.* **1992**, *30*, 569.
(34) Quiram, D. J.; Register, R. A.; Marchand, G. R. *Macromolecules* **1997**, *30*, 4551.
(35) Yang, Y.-W.; Tanodekaew, S.; Mai, S.-M.; Booth, C.; Ryan, A. J.; Bras, W.; Viras, K. *Macromolecules* **1995**, *28*, 6029.
(36) Strobl, G. *The Physics of Polymers: Concepts for Understanding their Structures and Behavior*; Springer: Berlin, 1996.
(37) Huo, P.; Cebe, P. *Colloid Polym. Sci.* **1992**, *270*, 840.
(38) Blundell, D. J.; Osborn, B. N. *Polymer* **1983**, *24*, 953.
(39) Adams, J. L.; Quiram, D. J.; Graessley, W. W.; Register, R. A.; Marchand, G. R. *Macromolecules* **1998**, *31*, 201.

MA049143M